Patel, D. J. (1975) *Biochemistry 14*, 3984–3989.
Patel, D. J. (1978) *Eur. J. Biochem. 83*, 453–464.
Patel, D. J., & Hilbers, C. W. (1975) *Biochemistry 14*, 2651–2656.
Patel, D. J., & Canuel, L. (1976) *Proc. Natl. Acad. Sci. U.S.A. 73*, 674–678.
Perrin, F. (1934) *J. Phys. Radium 5*, 497.
Rill, R. L., Hilliard, P. R., Jr., Bailey, J. T., & Levy, G. C. (1980) *J. Am. Chem. Soc. 102*, 418–420.
Selsing, E., Wells, R. D., Early, T. A., & Kearns, D. R. (1978) *Nature (London) 275*, 249–250.
Teitelbaum, H., & Englander, S. W. (1975) *J. Mol. Biol. 92*, 55–78.
Woessner, D. E. (1962) *J. Chem. Phys. 37*, 647–655.

A 300-MHz Proton Nuclear Magnetic Resonance Investigation of Deoxyribonucleic Acid Restriction Fragments: Dynamic Properties†

Thomas A. Early,‡ David R. Kearns,* Wolfgang Hillen,§ and Robert D. Wells

ABSTRACT: The 300-MHz relaxation behavior of the imino protons in Watson–Crick base pairs has been investigated in two DNA restriction fragments 43 and 69 base pairs (bp) in length over temperatures ranging from 18 to 59 °C. These results, in conjunction with data obtained on a 12-bp fragment, provide information on the nature of internal motions in the DNA and on the mechanism by which imino protons exchange with the solvent. Because the correlation time for axial rotation is much shorter than the correlation time for end-over-end tumbling, theory shows that the relaxation behavior of the imino protons is relatively insensitive to torsional modes but is very sensitive to end-over-end tumbling and bending modes. The "effective" end-over-end rotational correlation times required to fit the NMR relaxation data, 85 and 226 ns, are considerably shorter than the values, 150 and 490 ns, calculated for rigid cylinders 43 and 69 bp in length, respectively. The short effective rotational correlation times in these DNA are attributed to elastic bending modes which reorient the planes of the bases with respect to the helix axis. At elevated temperatures, the spin–lattice relaxation rates are dominated by exchange with the solvent, and measurements in this region can be used to investigate various aspects of the mechanism of breathing. The combined studies of the 12-, 43-, and 69-bp DNA demonstrate that the exchange of the T imino protons occurs by a single base-pair opening mechanism which is little affected by the DNA length or the neighboring base sequence. The activation energy of the process, 15.7 kcal, is relatively high and can probably be attributed to steric restraints imposed by the backbone. The close correspondence between the results obtained with the DNA restriction fragments and those obtained with poly(A)·poly(U) suggests that a common breathing mechanism is involved.

Proton nuclear magnetic relaxation techniques have been widely used in the investigation of the structures and conformational dynamics of small molecules (Noggle & Schirmer, 1971; Zens et al., 1976), but until recently they have been little used in studies of DNA. The few proton studies that have been reported (Early & Kearns, 1979; Hogan & Jardetzky, 1979, 1980) have been limited to studies of the relaxation behavior of the nonexchangeable protons using D_2O as the solvent. In recent papers (Early et al., 1980a,b), we demonstrated that the long-pulse method can be used to measure the spin–lattice and spin–spin relaxation rates of exchangeable protons in H_2O. In the preceding paper (Early et al., 1981), where we studied a 12-bp DNA restriction fragment (sequence shown in Table I), we have shown how measurements on the relaxation behavior of the imino protons in Watson–Crick base pairs can provide insight into the static and dynamic properties of the DNA double helix. The low-temperature spin–spin and spin–lattice relaxation rates in this 12-bp fragment are well predicted by using a relaxation theory in which the DNA helix is treated as a rigid rotor, indicating that insofar as relaxation of the low-field resonances is concerned, this short DNA fragment can be considered to be rigid on a time scale of 10 ns. However, in studies of larger DNA molecules (Early & Kearns, 1979; Early et al., 1980a), we found evidence, based on line-width considerations and relaxation measurements, for flexibility in the DNA indicating reorientation of the base-pair planes with time constants shorter than 200 ns. Consequently, one goal of the present study was to examine intermediate-sized molecules to determine where internal motions in the DNA begin to be important relative to the overall tumbling of the molecule.

A second point of interest in these studies concerns the mechanism by which A·T and G·C base pairs open and allow the imino protons to exchange with the solvent. These data are of particular interest in connection with theoretical studies of DNA melting (Tong & Battersby, 1979; Azbel, 1980) and may be important to the high-temperature flexibility of DNA (Godfrey & Eisenberg, 1976). Information on this point can be obtained from measurements of the relaxation rates of the imino protons obtained at sufficiently high temperatures so that exchange contributions to the relaxation are important.

† From the Department of Chemistry, University of California, San Diego, La Jolla, California 92093 (T.A.E. and D.R.K.), and the Department of Biochemistry, College of Agricultural and Life Sciences, University of Wisconsin, Madison, Wisconsin 53706 (W.H. and R.D.W.). *Received November 25, 1980.* This work was supported by the American Cancer Society (Grant CH 32 to D.R.K.), the National Science Foundation (Grants PCM-7911571 to D.R.K. and PCM-15033 to R.D.W.), and the National Institutes of Health (Grant CA 20279 to R.D.W.). W.H. was supported, in part, by the Max Kade Foundation and the Deutsche Forschungsgemeinschaft.

‡ Present address: Department of Chemistry, Colorado State University, Fort Collins, CO 80523.
§ Present address: Institut für Organische Chemie und Biochemie, Technische Hochschule, 6100 Darmstadt, West Germany.

0006-2960/81/0420-3764$01.25/0

Table I: Sequences of the Three DNA Restriction Fragments Derived from a *Hae*III Digest of pVH51

base pairs	sequence[a]
12	5′ CCGCACTGATGG 3′
43	5′ CCTTCTTCCTGTTCCTGGTCTTTTGCTCACATGTTCTTTCCGG 3′
69	5′ CCTGTTCATCTGCGTCCAGTTCGTTGAGCTTCTCCACGACCGTTAATGTCTGGCTTCTGATAAAGCGGG 3′

[a] 5′ to 3′.

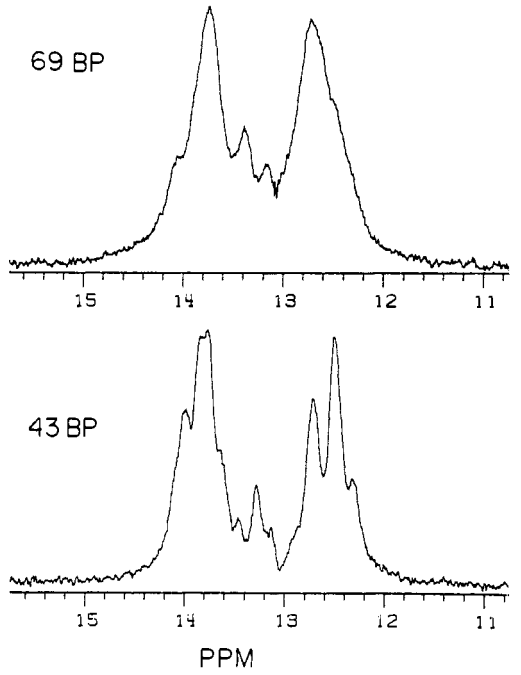

FIGURE 1: Low-field NMR spectrum (300 MHz) of a 43- and 69-bp DNA restriction fragment at 34 °C. The samples contained either 2.0 (43 bp) or 2.8 (69 bp) mg of DNA in 0.120 mL of solvent containing 0.33 M NaCl, 83 mM phosphate, and 0.17 mM EDTA at pH 7.3.

From our study of a 12-bp DNA restriction fragment, we obtained information on the opening rates of the four individual A·T base pairs in that molecule and concluded that similar rates should be observed in higher molecular weight DNA. In the present study, we have examined the relaxation behavior of DNA fragments containing 43 and 69 bp, with the sequences shown in Table I. The data on these fragments in conjunction with the data on the 12-bp DNA demonstrate that the rate of exchange of the thymine imino protons is independent of the DNA length and sequence and that a common activation energy can be used to account for the temperature dependence of the exchange rates in the three molecules. The mechanistic implications of these findings will be considered.

Materials and Methods

The three restriction fragments were isolated from a *Hae*III restriction enzyme digest of a pVH51 plasmid as described by Hillen et al. (1981). For the NMR experiments, 1.5, 2.0, and 2.8 mg, respectively, of the 12-, 43-, and 69-bp fragments were dissolved in 2.0 mL of solution and exhaustively dialyzed vs. 20 mM NaCl, 5 mM phosphate, and 0.01 mM ethylenediaminetetraacetic acid (EDTA) at pH 7.3. The samples were evaporated to dryness on a rotary evaporator, redissolved in 0.120 mL of doubly distilled water, and transferred to special Wilmad 508cp NMR tubes. With the 16.7-fold concentration, the final buffer concentration was 0.33 M NaCl, 83 mM phosphate, and 0.17 mM EDTA at pH 7.3.

Low-field NMR spectra were obtained on a spectrometer utilizing a Varian HR 300 magnet and probe and home-built

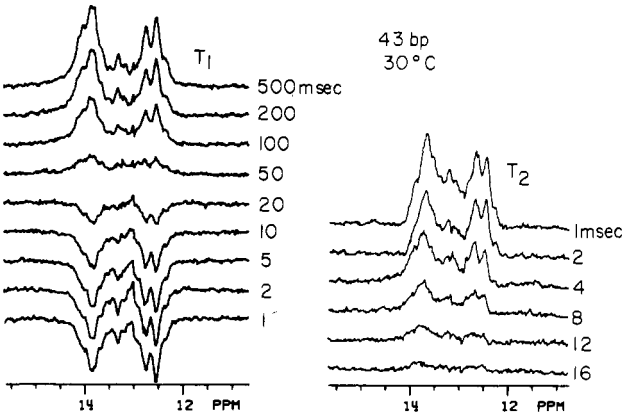

FIGURE 2: Example of a spin–lattice and spin–spin relaxation rate measurement on the low-field resonances of the 43-bp fragment. The temperature was maintained at 30 ± 1 °C. The long-pulse method was used (Early et al., 1980a), and the experimental conditions are similar to those used for the 12-bp fragment (Early et al., 1980b).

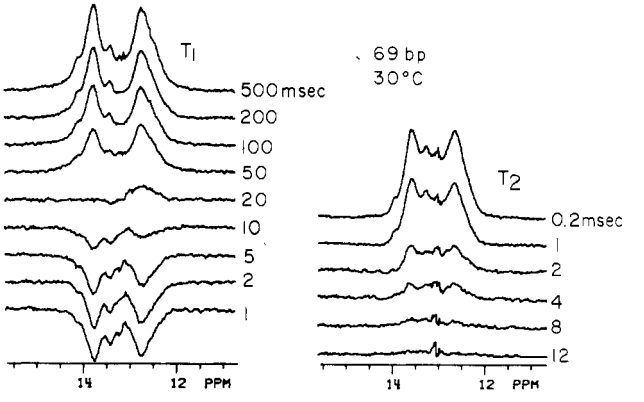

FIGURE 3: Spin–lattice and spin–spin relaxation rate measurements on the low-field resonances of the 69-bp fragment. For additional or experimental details see Early et al. (1980a, 1981).

FT electronics. The long-pulse method was used to make relaxation measurements (Early et al., 1980a).

Results

The low-field spectra of the 43- and 69-bp restriction fragments at 34 °C are shown in Figure 1. Although resonances from individual protons are generally not resolved under these conditions, most of the G·C and A·T resonances are well separated from one another, since A·T resonances are typically observed between 14.0 and ~13.0 ppm whereas G·C resonances are located between ~13.0 and 11.9 ppm (Kearns, 1977; Early et al., 1977; Patel & Canuel, 1976; Hilbers, 1979). The 43-bp fragment contains 21 G·C base pairs, and at 34 °C, we expect the resonances from the two terminal pairs to be lost due to rapid exchange with the solvent (Patel & Hilbers, 1975). We, therefore, expect a value of $^{22}/_{17} = 1.3$ for the ratio of the intensity of the A·T resonances relative to that of the G·C resonances, and experimentally we observe a value of 1.35. Since the spectrum of the 43-bp fragment exhibits partial resolution even at 300 MHz, we expect the 500-MHz spectrum to show even more structure.

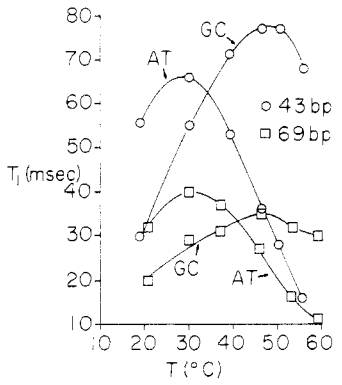

FIGURE 4: Plot of spin–lattice (T_1) relaxation times vs. temperature for the A·T and G·C resonances of the 43- and 69-bp fragments.

Examples of the inversion–recovery and spin–echo measurements are shown in Figures 2 and 3, and from these measurements, the spin–lattice ($T_1 = 1/R_1$) and spin–spin ($T_2 = 1/R_2$) relaxation times and rates are obtained for the low-field imino proton resonances at various temperatures. These results are shown in Table II, along with the corresponding data for the 12-bp fragment, and they are plotted in Figure 4.

The relaxation times for the various peaks in the spectra of the three fragments all exhibit qualitatively the same temperature dependence. As the temperature is increased from low temperature, the spin–lattice relaxation times initially increase, reach a maximum at some intermediate temperature, and then decrease at higher temperature until the resonances being monitored can no longer be detected. The maxima in T_1 occur at different temperatures depending upon the type of resonance monitored (A·T or G·C) and the size of the molecule. Excluding resonances from terminal base pairs of the 12-bp DNA, the T_1 maxima for the 12-, 43-, and 69-bp DNA occur at 45 ± 5 °C for the G·C base pairs and 25 ± 5 °C for the A·T base pairs. The magnitudes of the relaxation times, T_1, at any given temperature for the three fragments follow the order $T_1(12) > T_1(43) > T_1(69)$ for both the A·T and G·C resonances.

Spin–spin relaxation times, T_2, were measured at different temperatures, and these results are also given in Table II. For any given resonance, the maximum in T_2 was always observed at a higher temperature than the T_1 maximum. For the two larger DNA fragments, the low-temperature relaxation times are, at best, only estimates because the observed times are so short that appreciable relaxation occurs during the 1.2 ms required for the pulse sequence. With this R_f pulse duration, relaxation times shorter than 10 ms cannot accurately be measured.

Discussion

Relaxation data for the imino protons obtained at several temperatures for the 12-, 43-, and 69-bp DNA are summarized in Table II and in Figure 4. Qualitatively, the resonances in all three molecules exhibit the same temperature dependence. As the temperature increases, the relaxation rate decreases to a minimum and then increases until the resonance broadens beyond detection. As noted elsewhere (Early et al., 1980b, 1981), theoretical analysis shows that in the slow motion limit, where $\tau_1\omega > 1$, the selective relaxation rates are proportional to molecular tumbling times, τ_1, and therefore the product RT/η (R is a relaxation rate, R_1 or R_2, T is the absolute temperature, and η is the viscosity of pure water) should remain constant as long as other nonmagnetic effects do not contribute to the overall relaxation rate. Values of the product

Table II: Relaxation Rates (s^{-1}) for the Imino Protons of the 12-, 43-, and 69-bp Fragments at Various Temperatures[a]

temp (°C)	sample (bp)	R_1 (s^{-1}) A·T	R_1 (s^{-1}) G·C	R_2 (s^{-1}) A·T	R_2 (s^{-1}) G·C	RT/η[b] × 10^{-3}
1	12	11.7	15.3			2.4
5	12	7.7	12.7			2.3
8.5	12	6.3	9.3			1.9
11.5	12	5.5	8.1			1.8
14.5	12	4.9	6.3			1.5
18	12	4.9	6.0	29.9	32.7	1.6
21	12	5.0	5.3	23.2	25.3	1.6
24	12	5.5	4.8			1.5
28	12	6.4	4.4			1.6
32.5	12	9.3	4.2			1.7
35	12	12.9	4.3			1.8
38	12	15.9	4.5	19.6	10.6	2.0
18	43	18	33	131	135	35
30	43	15	18	85	100	38
38	43	18	14	85	77	35
47	43	27	13	71	59	31
51	43	35	13	83	64	38
56	43	62	14	99	58	38
21	69	31	50	303	323	97
30	69	25	34	263	270	103
37	69	27	32	149	167	75
46	69	37	28	141	147	80
53	69	62	31	143	121	76
59	69	90	33	170	111	78

[a] The observed values have an error limit of ±10%, except where the rates are >100 s^{-1}, in which case the error limits are ±50%. [b] The viscosity of pure water was used (Hardy & Cottingham, 1949). For the 12-bp fragment, R was the spin–lattice relaxation rate for the G·C resonances, whereas, for the 43- and 69-bp fragments, R was the spin–spin relaxation rate for the G·C resonances.

RT/η for the three DNA fragments are presented in Table II. The data indicate that the quantity RT/η remains reasonably constant over a range of temperatures, but at lower temperatures, it is unexpectedly high due to an increase in the nuclear relaxation rates. This increase in relaxation rates at low temperatures is due to a decrease in molecular tumbling rate (increase in tumbling time) which is attributed to intermolecular association at low temperatures. However, in the regime where the product RT/η becomes constant, aggregation is not important. For the 12-bp fragment, the product is constant from 18 to 35 °C, and for the 69-bp molecule, it becomes constant slightly above 30 °C. At high temperatures, the product R_2(G·C)T/η again increases for the 12-bp fragment because of exchange of the imino proton with the water solvent. In this high-temperature regime, where exchange with solvent is fast, the nuclear relaxation rate of an imino proton resonance is a direct measure of the exchange rate with the water, as will be discussed later. We now consider the factors which contribute to the nuclear relaxation at low temperatures.

(1) Analysis of the Magnetic Contributions to Relaxation. The magnetic contributions to the relaxation of a nuclear spin I by a second spin S are given by (Abragam, 1978)

$$R_1 = \frac{\gamma_I^2\gamma_S^2\hbar^2S(S+1)}{12r^6}[J_0(\omega_I - \omega_S) + 18J_1(\omega_I) + 9J_2(\omega_I + \omega_S)] \quad (1)$$

and

$$R_2 = \frac{\gamma_I^2\gamma_S^2\hbar^2S(S+1)}{24r^6}[4J_0(0) + J_0(\omega_I - \omega_S) + 18J_1(\omega_I) + 36J_1(\omega_S) + 9J_2(\omega_I + \omega_S)] \quad (2)$$

where R_1 is the spin–lattice relaxation rate of the I spins

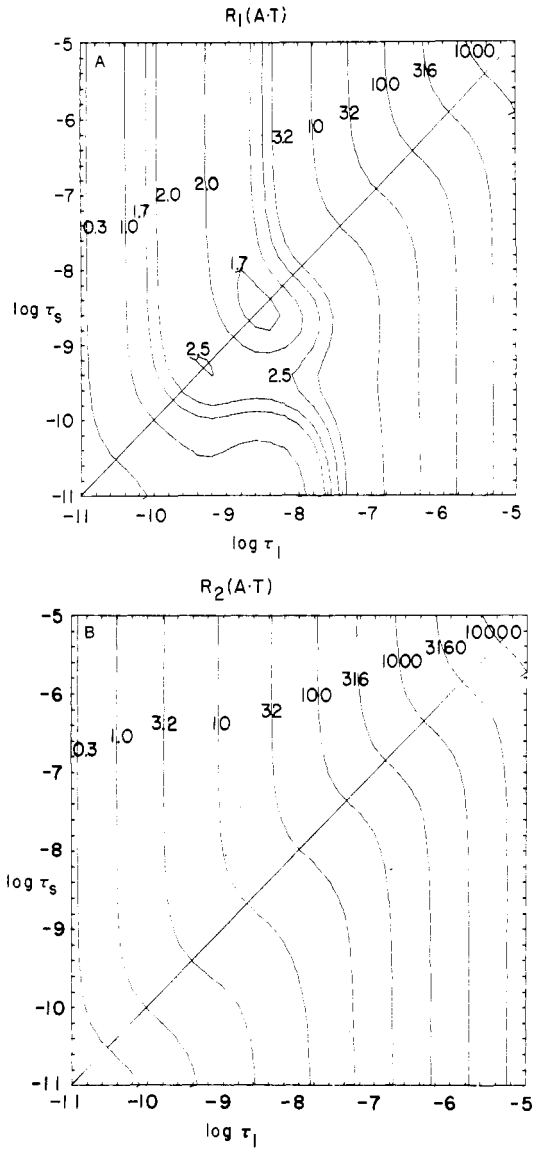

FIGURE 5: (A) Magnetic contributions to the spin–lattice (R_1) relaxation rate (s^{-1}) calculated by using eq 1 for all combinations of end-over-end (τ_1) and axial (τ_s) rotational times from 10 ps to 10 μs for an A·T base pair. Relaxation rates have been isocontoured on this two-dimensional grid of correlation times. Relaxation maps for G·C pairs are similar to the A·T maps and are not shown. For a further discussion of these maps, see the text. (B) Spin–spin (R_2) relaxation rates calculated by using eq 2 plotted on a grid of rotational correlation times.

resulting from a *selective* application of a 180° pulse to just the I spins, R_2 is the corresponding spin–spin relaxation rate, r is the I–S internuclear separation, γ_I and γ_S are the magnetogyric ratios of the I and S spins, and $J_n(\omega)$ is the spectral density at frequency ω resulting from molecular motions which modulate the I–S dipolar interaction. When more than one spin contributes to the relaxation of the I spin, the total relaxation rate will be the sum of contributions from each spin. If we assume that the overall motions of the DNA helix can be characterized by two rotational correlation times, τ_s, the correlation time for axial rotation, and, τ_1, the correlation time for end-over-end tumbling, and assume that internal motions of the base pairs are of sufficiently small amplitude and low frequency that the relaxation process can be treated by a rigid rotor model, then the theory developed by Woessner (1962) can be used to calculate the spectral densities, $J_n(\omega)$, needed in eq 1 and 2 and the corresponding relaxation rates. We have calculated R_1 and R_2 for various possible values of τ_1 and τ_s, and these results are shown in Figure 5. In this particular

Table III: Observed Spin–Lattice and Spin–Spin Relaxation Rates for the 43- and 69-bp Molecules at 30 °C Compared with Those Calculated by Using the Broersma Formula

sample (bp)		relaxation rates (s^{-1}) A·T R_1	A·T R_2	G·C R_1	G·C R_2	length (Å)	τ_1[d] (ns)
43	obsd	15	85	18	100	146[a]	85
	calcd[b]	15 ± 1	85–110	15	93–120	120[c]	
69	obsd	25	263	34	270	234[a]	226
	calcd[b]	25 ± 1	180–250	34	210–280	182[c]	

[a] Contour length of the molecule. [b] Calculated by using eq 1 or 2 with a helix radius of 13 Å, viscosity of 0.01 P, temperature of 303 K, and a helix length adjusted to best fit the observed values. Exchange contributions have been included in the A·T rates (7 ± 1 s^{-1} at 303 K). The range of calculated R_2 rates is without or with neighboring imino proton interactions. [c] The cylinder length required to fit the observed rotational correlation time. [d] The effective rotational correlation time determined from the NMR data and the $R_{1,2}$ maps.

representation, calculated relaxation rates have been isocontoured on a two-dimensional grid of rotational correlation times ranging from 10 ps to 10 μs. Values for an isotropic rotor ($\tau_1 = \tau_s$) appear along the diagonal whereas the relaxation rate values for prolate shapes (long cylinders) with $\tau_1 > \tau_s$ fall below the diagonal. The plots show that for the case where $\tau_1 \gg \tau_s$ the calculated relaxation rates are very sensitive to the end-over-end tumbling time but almost independent of the axial spinning rate. This is unfortunate since it implies that, in this regime, no information can be derived about the axial spinning and/or internal torsional motions of the DNA. However, due to the strong dependence of relaxation rates on end-over-end tumbling, precise information can be obtained on the *effective* end-over-end tumbling times for the 43- and 69-bp fragments. With this in mind, a graphical method has been developed for extracting an effective end-over-end correlation time from the nuclear relaxation data. In this method, the R_1 and R_2 maps are superimposed, and appropriate τ_1 and τ_s values which simultaneously predict the observed spin–lattice and spin–spin relaxation for both the A·T and G·C resonances are determined. The effective end-over-end correlation time for the 43- and 69-bp molecules were found to be 85 ± 12 and 226 ± 34 ns, respectively (see Table III), and it is reassuring to note that for these two molecules the set of rotational correlation times required to fit the R_1 and R_2 data lie in the prolate regime of the plot. This eliminates the very unlikely possibility that the effective end-over-end tumbling rate is faster than the axial spinning rate. The effective rotational correlation time derived from the NMR relaxation behavior will be identical with the overall molecular rotational correlation time only if the DNA molecule is rigid. However, if the molecule is flexible, due to elastic deformations, the effective NMR correlation time will be shorter than the overall tumbling time. Rotational correlation times have not been measured for very short DNA, but transient electric field experiments have been used to study molecules in the 110–250-bp range (Hogan et al., 1978; Hagerman, 1981), and it is found that the observed rotational correlation times in low salt are accurately predicted by the Broersma formula (Broersma, 1980) for rigid cylinders of length L and radius b

$$\tau_1^{-1} = \frac{18kT}{\pi\eta L^3}\left[\ln(L/b) - 1.57 + 7\left(\frac{1}{\ln(L/b)} - 0.28\right)^2\right] \quad (3)$$

where η is the solvent viscosity and T the temperature. Since

the molecules which we studied are substantially shorter than the persistence length of DNA, which is on the order of 500 Å (Harrington, 1978; Godfrey & Eisenberg, 1976), the Broersma formula should accurately predict τ_1. What we find, however (see Table III), is that the effective rotational correlation times of 85 and 226 ns determined by NMR are shorter than those calculated (150 and 490 ns) by using the true contour length of the DNA with the Broersma formula. For reduction of the calculated rotational correlation times, the "effective length" of the DNA that must be used in the Broersma formula is shorter than the true contour length by 20 ± 2% for both the 43- and 69-bp DNA. Therefore, assuming the semiempirical Broersma formula correctly predicts the overall tumbling rates for rigid systems, these data indicate that the 43- and 69-bp molecules are beginning to exhibit some degree of flexibility and can no longer be considered rigid rods. Since DNA is known to be an elastic molecule, we attribute this flexibility to elastic bending modes which reorient the planes of the base pairs with respect to the helix axis (Barkley & Zimm, 1979). Because of the very substantial length effect on the relaxation rates (factor of about 12 in going from 12 to 69 bp), we suggest that large amplitude, fast local reorientations of the planes of the bases are not involved. This does not apply to the backbone which is believed to be undergoing substantial motion on a very short (nanosecond) time scale (Early & Kearns, 1979, 1980b; Hogan & Jardetzky, 1979, 1980; Bolton & James, 1980).

(*2*) *High-Temperature Relaxation Behavior: The Exchange Contribution.* At elevated temperatures, proton exchange with the solvent begins to make a significant contribution to the observed spin–lattice relaxation rate, R_1. In order to separately evaluate the magnetic and exchange contributions to R_1, we make use of the following considerations. By evaluation of eq 1 and 2, we find (Early et al., 1980b) that the magnetic contributions to the spin–spin relaxation rate, R_2, can be 5–15 times larger than that to the spin–lattice relaxation rate. Consequently, there is a range of temperatures where the spin–lattice relaxation rate will be dominated by exchange, but R_2 will be relatively unaffected. In this temperature range, R_{ex}, the exchange contribution to R_1, can be estimated by first calculating the expected magnetic contribution to R_1 and subtracting it from the observed R_1 as follows:

$$R_{ex} = R_1 - R_2(R_1/R_2)_{\text{low temp}} \qquad (4)$$

where $(R_1/R_2)_{\text{low temp}}$ is measured at low temperatures where exchange is not important to the overall relaxation. This assumes that there are no conformational changes in the molecular structure of the DNA over the temperature range considered.

At sufficiently high temperatures, spin–lattice relaxation of imino protons will be totally dominated by the exchange contribution, R_{ex}. On the basis of previous studies of the exchange properties of the bases, it is believed that exchange with solvent occurs every time a base pair opens and exposes the imino proton to the solvent (McConnell, 1978; Mandal et al., 1979; Teitelbaum & Englander, 1975). Therefore, the high-temperature relaxation rates provide a direct measure of the base-pair opening rates. From the high-temperature data on the A·T base pairs of the 12-, 43-, and 69-bp fragments, where spin–lattice relaxation rates are dominated by the imino proton exchange rate, it is possible to determine the activation energy for the process controlling the exchange of the imino protons. In Figure 6, the natural log of the spin–lattice relaxation rate has been plotted against the reciprocal of the absolute temperature. In the case of the 69-bp molecule, the magnetic contributions are large due to the slow end-over-end tumbling of the molecule, and the experimental relaxation data for this molecule were corrected (indicated on plot) to remove the magnetic contribution to the overall relaxation rate by using eq 4. It was not necessary to correct the 12- and 43-bp data because the magnetic terms are small compared to the exchange contribution. A least-squares fit of the data gives an activation energy of 15.7 ± 1.0 kcal/mol, and the exchange contribution to the relaxation rate for an A·T imino proton resonance at any temperature T can be described by

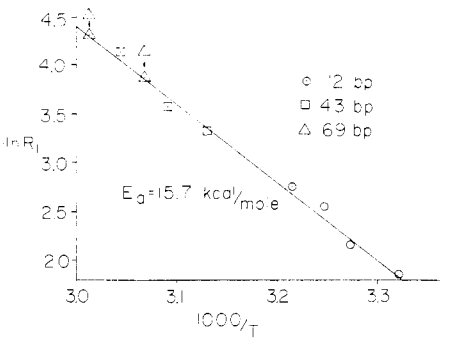

FIGURE 6: Natural log of the spin–lattice relaxation rates of the A·T resonances for three restriction fragments in the high-temperature limit where exchange dominates is plotted vs. the reciprocal of the absolute temperature. The 69-bp data have been corrected for the large magnetic contribution to the measured relaxation rate, and this is indicated on the plot.

$$R_{ex}(\text{A·T}) = [(1.2 \pm 0.2) \times 10^{12}]e^{-(7850\pm500)/T} \qquad (5)$$

This formula is not applicable to base pairs located at or near the end of the helix because these pairs are especially susceptible to exchange (Patel & Hilbers, 1975). Since the hydrogen-bond strength for an A·U base pair is only about 6 kcal (Binford & Holloway, 1968), the observed activation energy for exchange of the imino protons of individual A·T base pairs is surprisingly large. Perhaps, as has been suggested elsewhere (Mandal et al., 1979), this may be due to steric restrictions imposed by the backbone which make it difficult for a single base to swing out into the solvent while leaving the complementary base stacked.

The fact that the same equation (eq 5) can be used to predict the rate of exchange of the thymine imino protons with solvent in three different restriction fragments indicates that the mechanism by which exchange occurs is independent of the length of the DNA and the local sequence. This confirms our suggestion, on the basis of an analysis of the data from the 12-bp fragment, that opening of the A·T base pairs occurs by *single* base pair mechanisms, without opening of neighboring G·C base pairs. This is clearly indicated by the relaxation data shown in Figure 4 where we find that above 50 °C all of the A·T resonances in the 43- and 69-bp fragments relax faster by about a factor of 3 than do the G·C resonances in the same molecule whereas the reverse is true in the low-temperature region where magnetic contributions dominate the relaxation.

It is interesting to note that the activation energy and exchange rates of A·T base pairs derived from these DNA measurements are very close to the values obtained for poly(A)·poly(U) by using a stopped-flow technique (Mandal et al., 1979) in which changes in the optical density were monitored when the solvent was changed from H_2O to D_2O. Since the exchange rates and activation energy appear to be very similar to poly(A)·poly(U) and in the DNA fragments, we assume that the same mechanism is involved. The high activation energy for the exchange process was previously (Teitelbaum & Englander, 1976) attributed to a "rolling

bulge" mechanism in which melted regions of the duplex (bulge) travel down the helix and expose the imino protons to the solvent. For the three restriction fragments examined in this section, this interpretation is clearly not suitable.

Summary

In this paper, spin–lattice and spin–spin relaxation rate measurements on the low-field resonances of a 43- and 69-bp restriction fragments have been combined with data for a 12-bp restriction fragment (Early et al., 1981) in order to study the molecular motion of DNA in solution. Through the application of nuclear relaxation theory, in conjunction with Woessner's theoretical expressions for spectral densities (Woessner, 1962), the relaxation rate measurements are used to determine the effective rotational correlation times experienced by the base pairs in the DNA. The rotational correlation times deduced from the NMR data are shorter by about a factor of 2 than those estimated by using the Broersma (1960) formula for rigid cylinders of length corresponding to 43 and 69 bp, respectively. The NMR data, therefore, show clear evidence for flexibility in these molecules, even though they are significantly shorter than one persistence length (400–600 Å).

The nuclear relaxation behavior of the imino proton resonances at elevated temperatures shows that exchange of the thymine imino protons in the DNA with solvent occurs much faster than does exchange of neighboring guanine imino protons, and this is interpreted as a length- and sequence-independent opening of individual A·T base pairs with an activation energy of 15.7 kcal/mol for the process.

Acknowledgments

We thank Ron Behling for his help in carrying out some of the calculations.

References

Abragam, A. (1978) in *The Principles of Nuclear Magnetism*, p 57, The University Press, Oxford.

Azbel, M. Ya. (1980) *Biopolymers 19*, 61–80.

Barkley, M. D., & Zimm, B. H. (1979) *J. Chem. Phys. 70*, 2991–3007.

Binford, J. S., & Holloway, D. M. (1968) *J. Mol. Biol. 31*, 91–99.

Bolton, P. H., & James, T. L. (1980) *Biochemistry 19*, 1388–1392.

Broersma, S. (1960) *J. Chem. Phys. 32*, 1626–1631.

Early, T. A., & Kearns, D. R. (1979) *Proc. Natl. Acad. Sci. U.S.A. 76*, 4165–4169.

Early, T. A., Kearns, D. R., Burd, J. F., Larson, J. E., & Wells, R. D. (1977) *Biochemistry 16*, 541–551.

Early, T. A., Feigon, J., & Kearns, D. R. (1980a) *J. Magn. Reson. 41*, 343–348.

Early, T. A., Kearns, D. R., Hillen, W., & Wells, R. D. (1980b) *Nucleic Acids Res. 8*, 5795–5812.

Early, T. A., Kearns, D. R., Hillen, W., & Wells, R. D. (1981) *Biochemistry* (second paper of three in this issue).

Godfrey, J. E., & Eisenberg, H. (1976) *Biophys. Chem. 5*, 301–318.

Hagerman, P. (1981) *Biopolymers* (in press).

Hardy, R. C., & Cottingham, R. L. (1949) *NBS Handb. (U.S.) 42*, 573.

Harrington, R. E. (1978) *Biopolymers 17*, 919–935.

Hilbers, C. W. (1979) in *Biological Applications of Magnetic Resonance*, pp 1–43, Academic Press, New York.

Hillen, W., Klein, R. D., & Wells, R. D. (1981) *Biochemistry* (first paper of three in this issue).

Hogan, M. E., & Jardetzky, O. (1979) *Proc. Natl. Acad. Sci. U.S.A. 76*, 6341–6345.

Hogan, M. E., & Jardetzky, O. (1980) *Biochemistry 19*, 3460–3468.

Hogan, M. E., Dattagupta, N., & Crothers, D. M. (1978) *Proc. Natl. Acad. Sci. U.S.A. 75*, 195–199.

Kearns, D. R. (1977) *Annu. Rev. Biophys. Bioeng. 6*, 477–523.

Mandal, C., Kallenbach, N. R., & Englander, S. W. (1979) *J. Mol. Biol. 135*, 391–411.

McConnell, B. (1978) *Biochemistry 17*, 3168–3176.

Noggle, J. H., & Schirmer, R. E. (1971) in *The Nuclear Overhauser Effect: Chemical Applications*, Academic Press, New York.

Patel, D. J., & Hilbers, C. W. (1975) *Biochemistry 14*, 2651–2656.

Patel, D. J., & Canuel, L. (1976) *Proc. Natl. Acad. Sci. U.S.A. 73*, 674–678.

Teitelbaum, H., & Englander, S. W. (1975) *J. Mol. Biol. 92*, 55–78.

Tong, B. Y., & Battersby, S. J. (1979) *Biopolymers 18*, 1917–1936.

Woessner, D. E. (1962) *J. Chem. Phys. 37*, 647–655.

Zens, A. P., Bryson, T. A., Dunlap, R. B., Fisher, R. R., & Ellis, P. D. (1976) *J. Am. Chem. Soc. 98*, 7559–7564.